Int. J. Solids Structures, 1973, Vol. 9, pp. 1087 to 1105. Pergamon Press. Printed in Great Britain

# INITIAL-VALUE DISCRETE SUSPENSION BRIDGE ANALYSIS

HARRY H. WEST

Department of Civil Engineering, The Pennsylvania State University, University Park, Pennsylvania 16802

and

DANIEL L. CARAMANICO†

U.S. Army Engineer School Brigade, Ft. Belvoir, Virginia 22060

**Abstract**—A discrete formulation is presented for the analysis of suspension bridges. The resulting equations of equilibrium, which are nonlinear in the displacement terms, are solved by a Newton–Raphson procedure. The linear solution for each cycle of the Newton–Raphson method is treated as a set of linear initial-value problems. Numerical difficulties require that a suppression scheme be employed within each linearization. Numerical problems are presented for both stiffened and unstiffened structures and the results are compared with the findings of other investigators. The effects of hanger spacing on the results, especially in the end regions of the stiffening truss, are studied.

## 1. INTRODUCTION

SUSPENSION bridge analysis has received much attention over the years. Even though great suspension bridges are being designed and built with relative ease, studies continue because it affords the investigators an opportunity to understand the suspension bridge better and to gain insight into more complex cable-supported structures.

The early studies on suspension bridges during the nineteenth century culminated in the formulation of the "deflection theory" by Melan [1] in 1888. During the first half of the twentieth century, many authors [2–5] advanced methods for solving the basic equations of the deflection theory. These methods were generally designed for solution by hand or by a desk calculator. A period followed when several methods were presented that continued to treat the classical deflection theory but presumed the use of a digital computer. The more recent contributions [6–8], however, have considered more general formulations in which some of the restrictive assumptions of the classical deflection theory have been relaxed. This has not been done solely to get better results. Indeed, there is evidence that the nature of the assumptions made in the deflection theory did not jeopardize the results for most loading conditions. However, such assumptions involve artificial constraints that actually complicate the problem analytically. Thus, although relaxing the assumptions creates a larger computational problem, it simplifies the formulation of the problem. With the computer, a large computational problem is not necessarily detri-

† Formerly a graduate student at The Pennsylvania State University.

mental and the results will include all the "small" effects, which might be significant for certain loading cases.

West and Robinson [9] developed two separate methods of analysis. One was a discrete formulation requiring the solution of large numbers of nonlinear simultaneous algebraic equations, which made it somewhat undesirable from a computational point of view. The other was a continuous formulation in which the problem was expressed as a nonlinear boundary-value problem for ordinary differential equations. The differential equations were solved by an initial-value scheme [9, 10]. Although the latter method was the faster of the two computationally, the continuous model could not represent the structure as realistically as the discrete model could. Thus, it seemed reasonable to develop a scheme that would use a discrete model, which could accurately represent the structure, but solve the equations by an initial-value scheme. Such a method is presented in this paper.

It is shown that this method can be employed with a model having fewer than the actual number of hanger points to achieve excellent results. This is important for large bridges, or other large cable-supported structures, where the computational effort would be great if the structure is treated in full detail. However, care must be exercised in modeling the structure if erroneous results at the ends of the span are to be avoided.

In this paper, the derivation of the equations and the detailed algorithm for the solution of a single-span structure are presented. The general manner in which the equations would be applied to a three-span structure is also discussed. A few example problems are presented to illustrate the use of the method and to compare the results with those of other investigators.

## 2. DESCRIPTION OF MODEL STRUCTURE

The following items describe the structural model employed in this study:

1. The cable-hanger system is composed of discrete structural elements joined by frictionless pins at the hanger connection points along the main cable. Each element is assumed to be loaded uniaxially. Thus, the moment resisting capacity of the cable is neglected.
2. The stiffening member is treated as a beam in flexure. Shearing deformations are neglected, although they could be included with relative ease. Decks with variable moment of inertia are admissible.
3. The main cable is free to displace both vertically and horizontally within the plane of loading; however, the hanger bases, which attach to the stiffening member, are only free to displace vertically.
4. The effects of hanger elongations and hanger inclinations are included. Hangers are present at all node points along the cable except the anchorage and tower points.
5. The cable support systems at the tower and anchorage points are idealized as linear springs in the vertical and horizontal directions. However, the deck is assumed to have nonyielding vertical supports.
6. All materials are assumed to obey Hooke's Law. The geometric nonlinearity associated with the cable-hanger system is fully treated although the stiffening member is assumed to respond linearly to load.
7. The dead load configuration must be known or determined. For suspension bridges, the entire dead weight of the structure is assumed to be uniformly distributed along

the horizontal. Since this dead load is considered to be supported by the cable only, the cable assumes a parabolic configuration and the stiffening member is unstressed at mean temperature under dead load.

## 3. EQUATIONS OF CABLE-HANGER SYSTEM

A single-span cable-hanger system is shown in Fig. 1. The main cable elements and nodal points are associated with the index $i$ which ranges over $(n+1)$ node points and $n$ members. The indices $li$ and $bi$ are associated with the hangers and hanger base points, respectively. The $i$ for each of these indices corresponds to the point on the main cable from which the hanger is suspended and thus ranges from 2 to $n$. Applied loads are admissible at any of the nodal points along the cable or at the hanger bases.

An enlarged view of the three members framing into joint $i$ is shown in Fig. 2. Since in general, point $i$ could be a tower or anchorage point, springs are also included which represent the support restraints. The horizontal and vertical displacements resulting from

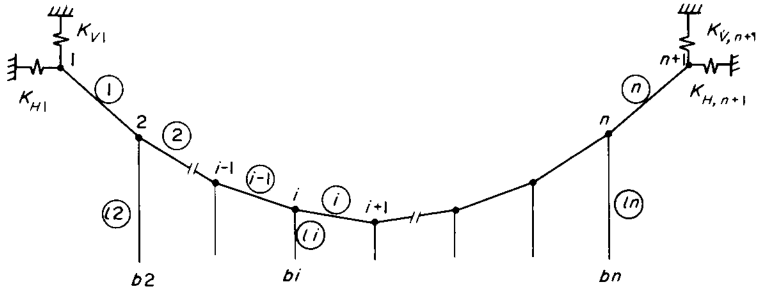


FIG. 1. Cable-hanger system.

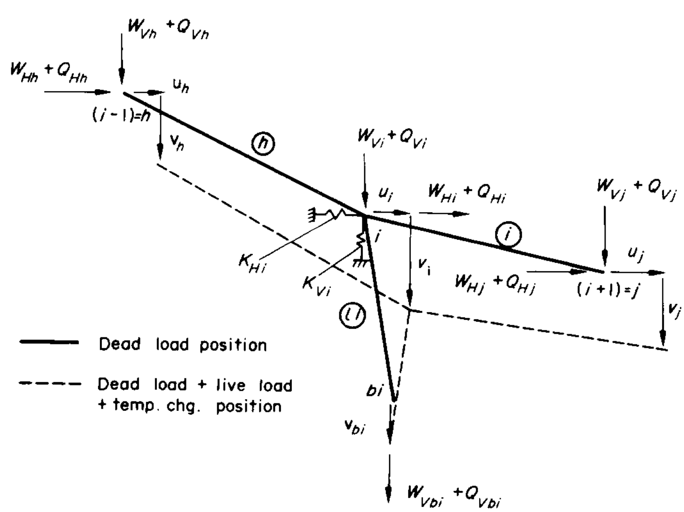


FIG. 2. Elements connecting to joint $i$.

live load and temperature changes are denoted by $u$ and $v$, respectively, with the subscript corresponding to the point at which the displacements are designated. The loads are also shown in Fig. 2. Live load is denoted by $Q$ and dead load by $W$ with the first subscript giving the direction of load ($H$ = horizontal, $V$ = vertical) and the second subscript identifying the point of application of the load. All displacements and loads are positive in the sense indicated in Fig. 2.

The final equations of equilibrium at station $i$ are derived in the Appendix. Equations (23) and (24) correspond to horizontal and vertical equilibrium, respectively, at point $i$ along the main cable, and equation (25) represents vertical equilibrium at the hanger base at point $bi$. As described in the Appendix, the right-hand sides of these equations simplify considerably if the initially assumed dead load configuration is in equilibrium under the actual dead load. The discussion here presumes that this is the case.

The equations of equilibrium of the Appendix are written in terms of the full load on the structure—live load and equivalent temperature load. In the application of these equations, the load term is not always the full load. Thus, in rewriting the equations of equilibrium below, the load terms $(Q_{Hi}+Q^t_{Hi})$, $(Q_{Vi}+Q^t_{Vi})$ and $(Q_{Vbi}+Q^t_{Vbi})$ are replaced by $T_{Hi}$, $T_{Vi}$ and $T_{Vbi}$, respectively. These loads will have different interpretations at different stages in the solution process. Thus, we have the following at point $i$:

$$-\alpha_h u_h+(\alpha_h+\alpha_i+\alpha_{li}+K_{Hi})u_i-\alpha_i u_j-\beta_h v_h+(\beta_h+\beta_i+\beta_{li})v_i-\beta_i v_j-\beta_{li}v_{bi}+N_{Hi} = T_{Hi} \quad (1)$$

$$-\beta_h u_h+(\beta_h+\beta_i+\beta_{li})u_i-\beta_i u_j-\gamma_h v_h+(\gamma_h+\gamma_i+\gamma_{li}+K_{Vi})v_i-\gamma_i v_j-\gamma_{li}v_{bi}+N_{Vi} = T_{Vi} \quad (2)$$

$$-\beta_{li}u_i-\gamma_{li}v_i+\gamma_{li}v_{bi}+N_{Vbi} = T_{Vbi}. \quad (3)$$

In the above, $\alpha$, $\beta$ and $\gamma$ are stiffness quantities as defined in the Appendix, which are evaluated for the configuration to which the loads are applied. The subscript indicates the bar that the particular stiffness quantity is associated with. The quantities $K_{Hi}$ and $K_{Vi}$ are the elastic restraints in the horizontal and vertical directions, respectively, which are present when $i$ corresponds to a support point. The terms $N_{Hi}$, $N_{Vi}$ and $N_{Vbi}$ are terms which are nonlinear in the displacement quantities.

As will be explained later, the procedure used in solving equations 1–3 requires that these equations be linearized by setting $N_{Hi} = N_{Vi} = N_{Vbi} = 0$. The modified equations enable one to determine the displacements corresponding to a linear solution for the $T$ set of loads. Since in the initial-value scheme, the displacements $u_h$, $v_h$, $u_i$ and $v_i$ are either known or assumed, the linearized form of equations (1–3) can be solved for the three unknown quantities—$u_j$, $v_j$ and $v_{bi}$. The displacement $v_{bi}$ can be determined directly from equation 3 as

$$v_{bi} = \frac{1}{\gamma_{li}}[\beta_{li}u_i+\gamma_{li}v_i+T_{Vbi}]. \quad (4)$$

With $v_{bi}$ now known, equations (1) and (2) can be solved simultaneously for $u_j$ and $v_j$. In matrix form, this solution can be expressed in the following indicial form:

$$\begin{Bmatrix} u_j \\ v_j \end{Bmatrix} = \begin{Bmatrix} u_i \\ v_i \end{Bmatrix} + \frac{1}{(\alpha_i\gamma_i-\beta_i^2)}\begin{bmatrix} -\gamma_i & \beta_i \\ \beta_i & -\alpha_i \end{bmatrix}\begin{Bmatrix} \sum_m \alpha_m(\bar{u}_m-u_i)+\sum_m \beta_m(\bar{v}_m-v_i)-K_{Hi}u_i+T_{Hi} \\ \sum_m \beta_m(\bar{u}_m-u_i)+\sum_m \gamma_m(\bar{v}_m-v_i)-K_{Vi}v_i+T_{Vi} \end{Bmatrix} \quad (5)$$

where the index $m$ ranges over all the bars which frame into joint $i$ with the exception of bar $i$ (bars $h$ and $li$), and $\bar{u}_m$ and $\bar{v}_m$ are the horizontal and vertical displacements, respectively, at the end of bar $m$ which is removed from point $i$. Thus, for bar $h$, $\bar{u}_m = u_h$ and $\bar{v}_m = v_h$, while for hanger $li$, $\bar{u}_m = u_{bi} = 0$ and $\bar{v}_m = v_{bi}$.

The quantity $(\alpha_i\gamma_i - \beta_i^2)$ is the determinant of the stiffness matrix of the $i$th bar. For no temperature change, this can be shown to be equal to $K_i^2 e_{id}/L_{id}$ where $K_i$, $e_{id}$ and $L_{id}$ are the axial stiffness, elongation and length, respectively, of the $i$th bar in the configuration to which the load is being applied. It is thus seen that without some initial load on the structure, the displacements $u_j$ and $v_j$ are undefined. In other words, the $i$th element has no stiffness without some initial load.

Further study of equation (5) shows that the term $\sum_m \alpha_m(\bar{u}_m - u_i) + \sum_m \beta_m(\bar{v}_m - \bar{v}_i)$ is the horizontal load at point $i$ associated with deformations of bars $h$ and $li$. Similarly $\sum_m \beta_m(\bar{u}_m - u_i) + \sum_m \gamma_m(\bar{v}_m - v_i)$ is the vertical load input at point $i$ from member deformations. At support points, the spring deformations also induce forces at point $i$. Thus, the column vector in equation (5) contains the loads input at joint $i$ by either the deformation of members framing into joint $i$ or the applied loads at joint $i$.

## 4. EQUATIONS OF STIFFENING MEMBER

A segment of the stiffening member is shown in Fig. 3 along with the shear, moment and deflection diagrams for the indicated loading.

An initial-value scheme similar to that used by Newmark [11] is used to express the essential relationships for the stiffening member. In indicial form, these relationships are

$$V_i = V_{i-1} + R_i - P_i \tag{6}$$

$$M_{i+1} = M_i + V_i\lambda_i \tag{7}$$

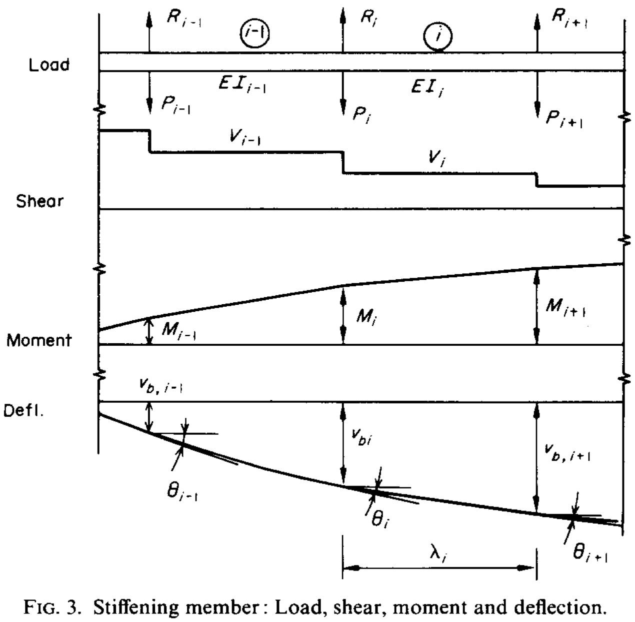


FIG. 3. Stiffening member: Load, shear, moment and deflection.

$$\theta_{i+1} = \theta_i - \frac{M_i\lambda_i}{EI_i} - \frac{V_i\lambda_i^2}{2EI_i} \tag{8}$$

$$v_{b,i+1} = v_{bi} + \theta_i\lambda_i - \frac{M_i\lambda_i^2}{2EI_i} - \frac{V_i\lambda_i^3}{6EI_i}. \tag{9}$$

In the above equations, $R$ is the upward hanger load, $P$ is the applied load and $V$, $M$, $\theta$ and $v_b$ are the shear, moment, slope and deflection of the stiffening member, respectively. The panel length is given by $\lambda$ and the member stiffness by $EI$. In all cases, the subscript refers to the panel or panel point being specified.

## 5. SOLUTION OF EQUATIONS

For an unstiffened suspension bridge, equations (1–3) must be satisfied for all points along the span. For a stiffened bridge, equations (6–9) must also be satisfied. In all equations, the load terms are understood to be the complete load (live + temperature) above some known equilibrium configuration. For either type of structure, the load–displacement relationships are nonlinear because of the influence of the cable. Thus, a direct solution of the governing equations is not possible and some iterative scheme must be employed.

*Newton–Raphson method*

The procedure used to solve the nonlinear equations is the Newton–Raphson Method. This is a well-known method for treating nonlinear problems with many degrees of freedom. The general technique is described by Livesley [12] and the specific application to the suspension bridge problem is discussed in detail by West and Robinson [9, 10]. The essential features of the method as it is applied to the unstiffened structure are briefly described below and portrayed graphically in Fig. 4. A series of linear solutions is carried

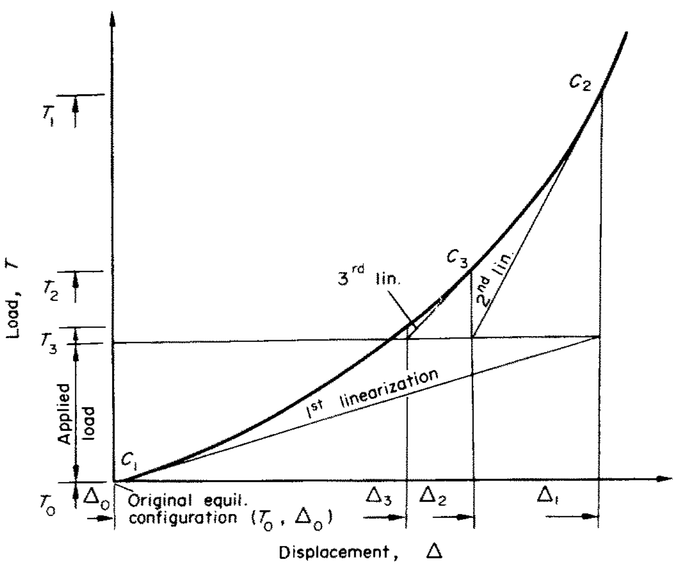


$C_i$ = Position on $T-\Delta$ curve corresponding to configuration for the $i$th linearization.

$T_i$ = Load corresponding to deformed configuration after $i$th linearization.

(Applied load $- T_i$) = Load for $(i+1)$th linearization.

$(\Delta_i - \Delta_{i-1})$ = Displacements corresponding to $i$th linearization.

$\Delta_i$ = Accumulated displacements after $i$th linearization.

FIG. 4. Newton–Raphson procedure.

out with the loads for each linearization being the difference between the known applied loads above the original equilibrium configuration and the loads corresponding to the current configuration. This set of loads is represented by the $T$ loads of equations (4) and (5). For each linear solution, the stiffness quantities used in equations (4) and (5) are evaluated for the deformed position about which the linearization is being performed. The loads corresponding to some deformed configuration are determined from equations (1–3) by using the stiffness quantities corresponding to the original equilibrium configuration and the accumulated displacements. Here, the resulting $T$ loads are the loads corresponding to this configuration. Eventually, after several linearizations, the loads for the next linearization approach zero and the deformed structure conforms to the known applied loads on the system.

In the above discussion, it has been implied that the full load is applied to the structure. In practice, it is best to segment the load. Each segment of load is treated as described above, with the original equilibrium configuration for the $i$th segment corresponding to the final equilibrium configuration for the $(i-1)$th segment.

*Linear solution*

Within the framework of the Newton–Raphson Method, it is necessary to determine the displacements corresponding to a set of loads using the linear equations. Each linear solution is treated as an initial-value problem. Two separate formulations are needed—one for the unstiffened structure and one for the stiffened structure.

(a) *Unstiffened suspension bridge.* For this case, equations (4) and (5) form the basis for a linear solution. A solution is initiated at point 1 by assuming cable displacements $u_1$ and $v_1$. Since no hanger is present at point 1, equation (4) is not needed. Equation (5) is also altered by the absence of the hanger $li$ and bar $h$ at point 1. Also, since point 1 is a support point, support springs are present and the load vector of equation (5) at point 1 becomes

$$\text{Load vector} = \begin{Bmatrix} -K_{H1}u_1 + T_{H1} \\ -K_{V1}v_1 + T_{V1} \end{Bmatrix}. \tag{10}$$

With this load vector, one can solve equation (5) for the displacements $u_2$ and $v_2$. It is now possible to solve for $v_{b2}$ from equation (4) and $u_3$ and $v_3$ from equation (5). Equations (4) and (5) are applied in this fashion for all $i$ values across the structure until one finally occupies station $n$ on the main cable from which $v_{bn}$ can be determined from equation (4) and $u_{n+1}$ and $v_{n+1}$ can be determined from equation (5).

It is unlikely that the displacements at the terminal point, $u_{n+1}$ and $v_{n+1}$, will satisfy the terminal boundary conditions. This is because the assumed displacements at the beginning point, $u_1$ and $v_1$, are not correct. Thus, there must be some scheme for modifying the beginning displacements such that the terminal boundary conditions are satisfied. This is accomplished by carrying three linear solutions simultaneously—one particular solution and two independent homogeneous solutions. The particular solution measures the effect of the load while the homogeneous solutions measure the effects of unit changes in the initially assumed displacements. The assumed initial displacements and loads for each solution are shown in Table 1, where $k = 0$ for the particular solution and $k = i$ for the $i$th homogeneous solution. The displacements and loads are bracketed and subscripted in accordance with the $k$ index. At the terminal point, these three solutions must

TABLE 1. INITIAL CONDITIONS AND LOADS FOR UNSTIFFENED SUSPENSION BRIDGE

| Solution | Initial displacements | | Loads | | |
|---|---|---|---|---|---|
| $k$ | $(u_1)_k$ | $(v_1)_k$ | $(T_{Hi})_k$ | $(T_{Vi})_k$ | $(T_{Vbi})_k$ |
| 0 | $(u_1)_0$ | $(v_1)_0$ | $(T_{Hi})_0$ | $(T_{Vi})_0$ | $(T_{Vbi})_0$ |
| 1 | $(u_1)_1$ | 0 | 0 | 0 | 0 |
| 2 | 0 | $(v_1)_2$ | 0 | 0 | 0 |

be combined in such a way as to satisfy the terminal boundary conditions. Thus we have

$$\sum_{k=1}^{2} C_k \begin{Bmatrix} (\Delta H_{n+1})_k \\ (\Delta V_{n+1})_k \end{Bmatrix} + \begin{Bmatrix} (\Delta H_{n+1})_0 \\ (\Delta V_{n+1})_0 \end{Bmatrix} = \begin{Bmatrix} (T_{H,n+1})_0 \\ (T_{V,n+1})_0 \end{Bmatrix} \tag{11}$$

where the quantities $(\Delta H_{n+1})_k$ and $(\Delta V_{n+1})_k$ are the horizontal and vertical forces, respectively, at the terminal point corresponding to the displacements for the $k$th linear solution. The values for $\Delta H$ and $\Delta V$ for each solution are determined from the linear part of the left-hand sides of equations (1) and (2), respectively, for $i = n+1$. These equations are somewhat simplified by the fact that the hanger $li$ and the bar $i$ are not present at joint $n+1$. However, since this is a support point, the support springs are present. Thus, we obtain

$$\begin{Bmatrix} (\Delta H_{n+1})_k \\ (\Delta V_{n+1})_k \end{Bmatrix} = \left[\begin{array}{c|c|c|c} -\alpha_n & \alpha_n + K_{H,n+1} & -\beta_n & \beta_n \\ \hline -\beta_n & \beta_n & -\gamma_n & \gamma_n + K_{V,n+1} \end{array}\right] \begin{Bmatrix} (u_n)_k \\ (u_{n+1})_k \\ (v_n)_k \\ (v_{n+1})_k \end{Bmatrix}. \tag{12}$$

Equations (11) are solved for $C_1$ and $C_2$. These constants indicate how much of each of the two homogeneous solutions must be added to the particular solution so that the forces at the terminal point are equal to those being applied for this linearization. These constants enable one to determine by superposition any quantity of the final solution, $S$, in terms of the corresponding quantities for the particular and homogeneous solutions.

$$S = (S)_0 + \sum_{k=1}^{2} C_k (S)_k. \tag{13}$$

At the end of a given linearization, the algebraic sums of the displacements for all linearizations are determined. These displacements are then substituted into the left-hand sides of equations (1–3) with all terms evaluated in terms of the original equilibrium configuration for this load segment. The resulting quantities are the loads corresponding to this deformed configuration. These loads are compared with the applied loads for this segment to determine whether another linearization is necessary.

(b) *Stiffened suspension bridge.* In addition to equations (4) and (5), equations (6–9) form the basis for a linear solution for the stiffened structure. A solution is begun at point 1 on the cable by assuming cable displacements $u_1$ and $v_1$. The displacements $u_2$ and $v_2$ are computed as for the unstiffened structure. The boundary conditions at the left end of the deck require that $M_1 = v_{b1} = 0$; however, the shear in the first panel, $V_1$, and the slope at the left support, $\theta_1$, must be assumed. On the basis of these initial values, $M_2$, $\theta_2$ and $v_{b2}$ are determined from equations (7–9), respectively, for $i = 1$.

For $i = 2$, we must first consider the base of the hanger. In addition to the load that may be applied at the hanger base for this linearization, $T_{Vbi}$, the load from the bridge deck, $R_i$, will also be applied at this point. This load must be added to the right-hand side of equation (3). Linearizing the modified equation (3) by setting $N_{Vbi} = 0$ and solving for $R_i$, we obtain

$$R_i = -\beta_{li}u_i - \gamma_{li}v_i + \gamma_{li}v_{bi} - T_{Vbi}. \tag{14}$$

Specifically, for $i = 2$, all is known in equation (14) but $R_2$. Solving for $R_2$, we can determine $V_2$ from equation (6) in which $P_2$ should be interpreted as the load applied to the deck for this linearization. The quantities $M_3$, $\theta_3$ and $v_{b3}$ are calculated from equations (7–9), respectively, while cable displacements $u_3$ and $v_3$ are determined from equation (5). This procedure continues across the span until finally, for $i = n$, one computes $u_{n+1}$ and $v_{n+1}$ on the cable and $M_{n+1}$ and $v_{b,n+1}$ on the deck.

As in the unstiffened structure, our assumptions at the beginning point are not likely to satisfy the terminal boundary conditions. In this case, we have the same force boundary conditions on the cable as for the unstiffened structure and, in addition, we have the deck boundary conditions that $M_{n+1} = v_{b,n+1} = 0$. Here, since we have a fourth-order system, four homogeneous solutions are carried along with the particular solution. The assumed initial conditions and loads for each solution are given in Table 2. Again, $k = 0$ for the

TABLE 2. INITIAL CONDITIONS AND LOADS FOR STIFFENED SUSPENSION BRIDGE

| Solution | Initial conditions | | | | Loads | | | |
|---|---|---|---|---|---|---|---|---|
| $k$ | $(u_1)_k$ | $(v_1)_k$ | $(V_1)_k$ | $(\theta_1)_k$ | $(T_{Hi})_k$ | $(T_{Vi})_k$ | $(T_{Vbi})_k$ | $(P_i)_k$ |
| 0 | $(u_1)_0$ | $(v_1)_0$ | $(V_1)_0$ | $(\theta_1)_0$ | Actual loading | | | |
| 1 | $(u_1)_1$ | 0 | 0 | 0 | 0 | 0 | 0 | 0 |
| 2 | 0 | $(v_1)_2$ | 0 | 0 | 0 | 0 | 0 | 0 |
| 3 | 0 | 0 | $(V_1)_3$ | 0 | 0 | 0 | 0 | 0 |
| 4 | 0 | 0 | 0 | $(\theta_1)_4$ | 0 | 0 | 0 | 0 |

particular solution and $k = i$ for the $i$th homogeneous solution. At the terminal point, the five solutions are combined to give

$$\sum_{k=1}^{4} C_k \begin{Bmatrix} (\Delta H_{n+1})_k \\ (\Delta V_{n+1})_k \\ (M_{n+1})_k \\ (v_{b,n+1})_k \end{Bmatrix} + \begin{Bmatrix} (\Delta H_{n+1})_0 \\ (\Delta V_{n+1})_0 \\ (M_{n+1})_0 \\ (v_{b,n+1})_0 \end{Bmatrix} = \begin{Bmatrix} (T_{H,n+1})_0 \\ (T_{V,n+1})_0 \\ 0 \\ 0 \end{Bmatrix}. \tag{15}$$

The quantities $(\Delta H_{n+1})_k$ and $(\Delta V_{n+1})_k$ are determined from equation (12). Equation (15) represents four simultaneous equations with unknowns $C_1$, $C_2$, $C_3$ and $C_4$. Solution of these equations for the constants enables one to superpose the five solutions for any quantity $S$ of the final solution.

$$S = (S)_0 + \sum_{k=1}^{4} C_k(S)_k. \tag{16}$$

At the end of a given linearization, the loads at the cable nodes corresponding to the deformed configuration are determined just as they were for the unstiffened structure by equations (1) and (2). When the accumulated displacements are substituted into the left-hand side of equation (3), the total loads at the base of the hangers for the deformed configuration are determined. Part of each of these loads is the load known to be applied to the hanger base for this linearization, $T_{Vbi}$. The remainder must be the load $R_i$, which comes from the deck. Since all panel shears are known for this linearization as determined from equation (16), the deck loads $P_i$, corresponding to the deformed configuration, can be determined from equation (6). The cable loads and deck loads for the deformed configuration are compared with the applied loads for this segment to determine whether another linearization is necessary.

*Numerical difficulties*

The initial-value formulation has some purely numerical problems associated with its application. These problems are not serious if they are understood, and a brief description of their nature is given in the following.

(a) *Suppression technique.* Even for reasonably good assumptions for the initial conditions, the displacements may reach the order of $10^{30}$ times the originally assumed values. This is because we are dealing with functions that grow in an exponential fashion. Since the computer can only carry a limited number of significant figures, this kind of growth is intolerable because round-off and truncation errors will make the results completely meaningless.

To limit the growth, a suppression scheme is used. This is similar to the method explained in detail by West and Robinson [9, 10]. The function of this technique is to keep the displacements within reasonable bounds. Whenever the displacements in either the particular or homogeneous solution exceed some acceptable magnitude, then a new particular solution and the required number of new independent homogeneous solutions are generated, each with specified displacements at the "suppressed" point. These new solutions are determined by combining the unsuppressed solutions to satisfy artificial internal boundary conditions. The advancement then continues across the span until suppression is again required. Eventually, at the terminal point, the particular solution is suppressed to the real boundary conditions as indicated in equations (11) and (15).

(b) *Initial and suppressed values.* The selection of the initial conditions indicated in Tables 1 and 2 is not completely arbitrary. Also, the artificial boundary conditions to which the particular and homogeneous solutions are suppressed must be selected with some care.

Consider first the unstiffened structure. If $(u_1)_0$ and $(v_1)_0$ in Table 1 for the particular solution are too large, then the forces induced by the spring deformations will effectively submerge the actual load at the first point because only a limited number of significant figures can be carried. If this occurs, then the particular solution no longer accurately reflects the load effects at the first point. This can be seen clearly by examining the load vector of equation (10), which becomes the load vector when equation (5) is applied at point 1.

Even for the homogeneous solutions, numerical difficulties are encountered if $(u_1)_1$ and $(v_1)_2$ of Table 1 are too large. In this case, the loads input from the springs at point 1 are very large and the resulting displacements at point 2 are huge. When suppression is then attempted at point 2, these homogeneous solutions cannot be combined to get "small" displacements because the truncation errors are larger than the displacements sought through suppression. The result is that the suppressed homogeneous solutions are not strongly independent.

Along the span, suppression must be performed whenever the displacements of any solution become large enough to cause numerical problems. At the terminal point, all solutions are suppressed before attempting to satisfy equation (11). If this is not done, the forces from the deformations of the terminal springs may be so large that the actual load at the terminal point may not be reflected in the final solution.

The stiffened structure displays the same kind of numerical problems as does the unstiffened structure. The same reasoning must be applied in treating these problems as has been outlined for the unstiffened structure.

*Miscellaneous notes*

For the sake of simplicity, the discussion thus far has centered about a single-span structure for which the initial configuration is known. These restrictions will now be removed.

(a) *Initial load configuration.* For a conventional suspension bridge, it is generally assumed that the dead load is constant along the horizontal and that the stiffening member is unstressed at dead load and mean temperature. For this case, the original dead load geometry and the forces in all elements of the cable system are easily obtained.

For cable systems having a more complicated dead load, the initial configuration is more difficult to determine. One way to proceed is to use some approximate scheme to determine an assumed initial shape and corresponding element forces. The question is, are these approximations consistent with the known dead load on the structure? This question can be answered by examining the right-hand sides of equations (23–25). For example, the bracketed term on the right-hand side of equation (23) is the sum of the horizontal components of forces in all the elements framing into point $i$. As pointed out in the Appendix, if the assumed initial configuration is consistent with the actual dead load, then this bracketed term will cancel $W_{Hi}$ exactly. If the assumed configuration is not consistent with the actual dead load, then the sum of the bracketed term and $W_{Hi}$ will yield a net horizontal load. Since initially $Q_{Hi}$ and $Q^t_{Hi}$ are zero, this net load constitutes the total load $T_{Hi}$ of equation (1). Similarly, $T_{Vi}$ and $T_{Vbi}$ of equations (2) and (3) are determined by examining the right-hand sides of equations (24) and (25), respectively. We now have a problem just like the live load problem. The resulting displacements establish the actual dead load configuration which becomes the initial configuration for live load.

Of course, if the dead load configuration is not desired, then the complete right-hand sides of equations (23–25) are taken as the loads $T_{Hi}$, $T_{Vi}$ and $T_{Vbi}$. The resulting displacements give the final position of the structure under dead load, live load and temperature load. These displacements are, of course, with respect to the initially assumed configuration.

(b) *Three-span structure.* Study of the three-span structure requires some additional considerations.

For the unstiffened structure, the analysis is the same as for the single-span structure except that there are internal points where support stiffness $K_{Hi}$ and $K_{Vi}$ exist. These points correspond to the tower locations and the stiffnesses are the horizontal and vertical stiffness of the tower.

For a stiffened structure, the cable system is handled in the same fashion as for the unstiffened structure. The manner in which the deck is treated depends on its support conditions at the tower. The important point is that equilibrium and compatibility be satisfied at the tower and that a sufficient number of independent homogeneous solutions emerge from the tower point to continue the initial-value scheme across the span.

For the sake of brevity, no three-span examples are presented here; however, no additional problems are encountered in their solution.

(c) *Fixed supports.* If the cable support points are actually fixed, two approaches are possible. In one, support stiffnesses are selected that are large enough to produce end displacements that are zero to the number of places being considered. Alternately, the computational scheme can be varied by actually setting the displacements at the left support equal to zero and beginning the initial-value problem by assuming the displacements at the second point. At the terminal point, the homogeneous and particular solutions are combined to satisfy the displacement boundary conditions on the cable rather than the force boundary conditions.

## 6. EXAMPLE PROBLEMS

In this section, the results of a few numerical problems are presented. The intent is to compare the results as determined from this method of analysis with those determined by other investigators.

*Example* 1

As a first example, an unstiffened structure with a large unsymmetrical load is treated. The structure and the total loading is shown in Fig. 5. This problem was first presented by Michalos and Birnstiel [13] and their results have subsequently been substantiated by other investigators [8, 14]. In the analysis presented here, the cable is divided into ten segments with the initially assumed configuration taken as that given by Michalos and Birnstiel. Since the response in this case is quite nonlinear, the load is divided into seven load segments. The number of linear solutions required for each segment ranges from six for the first load segment to two for the seventh load segment, with a total of 23 linearizations. The displacements are determined at all panel points and are given in Table 3.

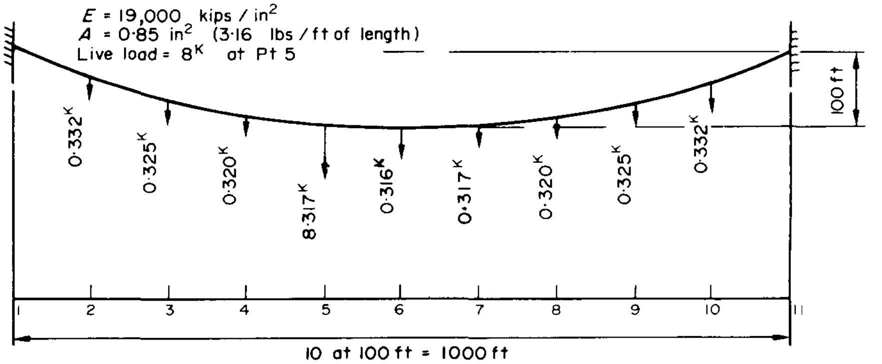


FIG. 5. Cable structure for Example 1.

TABLE 3. DISPLACEMENTS FOR EXAMPLE 1

| Point | Horizontal displacement (ft) | | Vertical displacement (ft) | |
|---|---|---|---|---|
| | Michalos and Birnstiel | West and Caramanico | Michalos and Birnstiel | West and Caramanico |
| 2 | 1·690 | 1·690 | −4·669 | −4·670 |
| 3 | 1·407 | 1·408 | −3·291 | −3·293 |
| 4 | −0·273 | −0·272 | 4·217 | 4·217 |
| 5 | −2·773 | −2·773 | 17·953 | 17·956 |
| 6 | −3·689 | −3·691 | −0·776 | −0·786 |
| 7 | −4·842 | −4·845 | −13·117 | −13·129 |
| 8 | −5·640 | −5·642 | −19·149 | −19·161 |
| 9 | −5·492 | −5·494 | −18·938 | −18·949 |
| 10 | −3·810 | −3·811 | −12·540 | −12·548 |

These displacements record the movement from the originally assumed configuration to the final configuration under the total loads. Table 3 also includes the results obtained by Michalos and Birnstiel. Excellent agreement is indicated.

*Example* 2

As an example of the analysis of a stiffened structure, the structure shown in Fig. 6 is investigated. The structure is divided into ten segments and a live load of 4 kips/ft is applied at the deck level across the entire span. Support stiffnesses are large, such that the cable displacements at the supports are zero to the number of places being reported. In this problem, the load is applied in two segments, and two linearizations are required for each load segment.

The final displacements and moments are reported in Table 4. This problem was also solved using a discrete method of analysis by West and Robinson [9]. Their results are also given in Table 4. The comparison between the two solutions is very good.

In the studies performed by West and Robinson [9, 10], it was shown that a discrete formulation of the suspension bridge which uses a small number of segments gives excellent results except in the area near the supports. In this region, the computed moments and end shear are too small. This is because the grid is too coarse to accurately measure the effects in this area. In their studies, they also solved a continuous formulation of the problem. However, this approach does not yield truly accurate results either since the continuous model provides for hangers all the way into the tower. This also does not

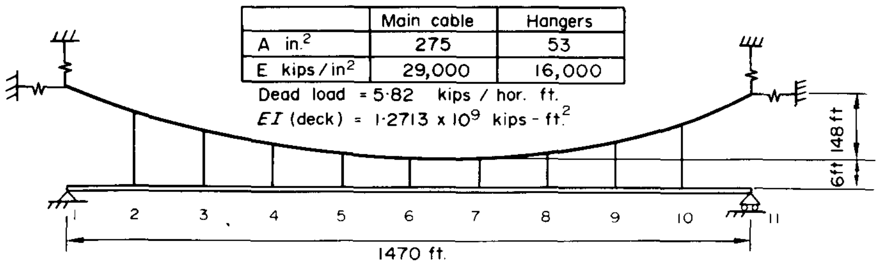


FIG. 6. Stiffened cable structure for Example 2.

TABLE 4. DISPLACEMENTS AND MOMENTS FOR EXAMPLE 2

| Point | Horizontal cable displacement (ft) | | Vertical cable displacement (ft) | | Vertical deck deflection (ft) | | Moment (Kip-ft.) | |
|---|---|---|---|---|---|---|---|---|
| | West and Caramanico | West and Robinson | West and Caramanico | West and Robinson | West and Caramanico | West and Robinson | West and Caramanico | West and Robinson |
| 2 | −0·140 | −0·138 | 0·802 | 0·797 | 0·869 | 0·880 | 7,390 | 7,660 |
| 3 | −0·219 | −0·219 | 1·582 | 1·585 | 1·623 | 1·643 | 10,700 | 10,900 |
| 4 | −0·206 | −0·206 | 2·178 | 2·184 | 2·199 | 2·222 | 12,800 | 13,000 |
| 5 | −0·122 | −0·122 | 2·551 | 2·558 | 2·559 | 2·583 | 14,100 | 14,200 |
| 6 | 0 | 0 | 2·677 | 2·684 | 2·681 | 2·706 | 14,600 | 14,500 |
| 7 | 0·121 | 0·122 | 2·550 | 2·558 | 2·559 | 2·583 | 14,100 | 14,200 |
| 8 | 0·205 | 0·206 | 2·178 | 2·184 | 2·198 | 2·222 | 12,800 | 13,000 |
| 9 | 0·219 | 0·219 | 1·582 | 1·585 | 1·622 | 1·642 | 10,700 | 10,900 |
| 10 | 0·139 | 0·138 | 0·802 | 0·797 | 0·868 | 0·880 | 7,350 | 7,660 |

correctly represent the real situation and gives moments and an end shear that are too large. The correct results can only be obtained with a discrete model having the correct hanger spacing. However, this entails a significant computational effort. Therefore, the procedure developed in this study is designed to allow for variable panel lengths. In this way, the hangers can be spaced correctly near the supports where it is necessary and spread out in the center of the span.

The structure of Example 2 has been solved by dividing the span into ten equal panels of 147 ft. The results for this are reported in Table 4. Three hangers at the correct spacing of 21 ft are now added at each end of the span to give a total of sixteen panels. Again, as was the case with ten panels, the load is applied in two segments, and two linearizations are required for each load segment. The vertical cable deflections and bridge deck moments at the tenth points of the span for the two solutions are compared in Table 5 to show that closing the spacing at the ends does not appreciably affect the results at these points.

Figure 7 shows the deck moments near the left support plotted for the continuous study of West and Robinson, the discrete study with ten equal panels and the discrete study with sixteen panels. The corresponding end shears are also given. Note that the

TABLE 5. RESPONSE OF STRUCTURE IN EXAMPLE 2 USING DIFFERENT PANEL LENGTHS

| Point | Ten equal panels | | Sixteen unequal panels | |
|---|---|---|---|---|
| | Vertical cable displacement (ft) | Moment (Kip-ft) | Vertical cable displacement (ft) | Moment (Kip-ft) |
| 2 | 0·802 | 7,390 | 0·806 | 7,370 |
| 3 | 1·582 | 10,700 | 1·589 | 10,700 |
| 4 | 2·178 | 12,800 | 2·185 | 12,900 |
| 5 | 2·551 | 14,100 | 2·558 | 14,100 |
| 6 | 2·677 | 14,600 | 2·684 | 14,600 |
| 7 | 2·550 | 14,100 | 2·557 | 14,100 |
| 8 | 2·178 | 12,800 | 2·184 | 12,800 |
| 9 | 1·582 | 10,700 | 1·588 | 10,700 |
| 10 | 0·802 | 7,350 | 0·805 | 7,320 |

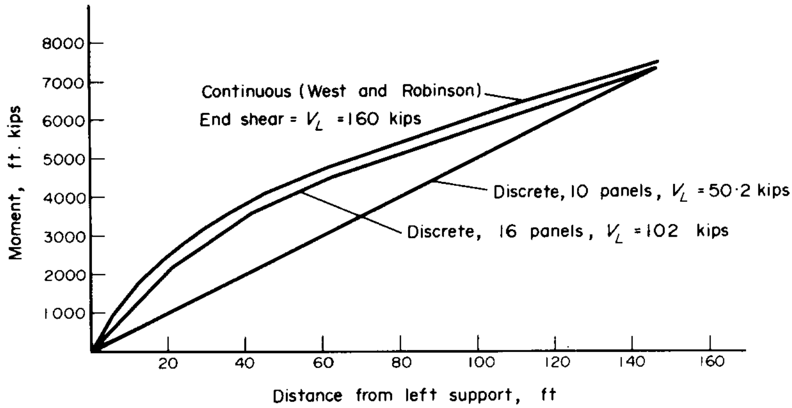


FIG. 7. Moments for Example 2 in left tenth of span.

results for the case of sixteen panels fall between those for the continuous system and the discrete model with ten panels. The fact that good results can be obtained near the supports without sacrificing the accuracy near the center of the span, makes this a valuable method. By using the correct hanger spacing near the towers and a coarser grid in the rest of the span, good results can be obtained without the added time and effort of using the correct spacing of hangers throughout.

## 7. CONCLUSIONS

It is shown that a suspension bridge can be analyzed using a discretized mathematical model to formulate the governing equations and an initial-value approach for solving these equations.

The equations of equilibrium, which are nonlinear in the displacement terms, are solved by a Newton–Raphson method with each cycle being treated as a set of linear initial-value problems. Numerical difficulties require that a suppression scheme be employed within each linearization. However, the method is still computationally faster than a discrete method which solves linear simultaneous algebraic equations for each cycle, unless a very large number of suppressions is needed.

The results of numerical problems agree well with the findings of previous investigators, both for unstiffened and stiffened structures. Previous studies have indicated that significant errors are introduced in the end regions of the stiffening truss when a discrete model with larger than actual hanger spacing is employed. It is demonstrated that this problem can be corrected by using the actual hanger spacing near the supports while maintaining a wider spacing throughout the interior portion of the span.

*Acknowledgements*—This paper is based on part of the research conducted by the senior author under a National Science Foundation Research Initiation Grant. At the time of this study, the junior author was studying under a National Science Foundation Traineeship. The authors are grateful for this support.

Thanks are also due to Arthur R. Robinson, Professor of Civil Engineering at the University of Illinois, who participated in the early conception of the study and who offered suggestions throughout. The authors are also grateful to Anil K. Kar, who worked on another phase of this research effort and offered much technical assistance.

## REFERENCES


[1] J. MELAN, Theorie der eisernen Bogenbrucken und der Hangebrucken. *Handbuch der Ingenieurwissenschaften*. 2nd edition (1888).

[2] S. O. ASPLUND, On the deflection theory of suspension bridges. *Ingenjorsvetenskapsakademins Handlinger*, **184** (1945).

[3] A. A. JAKKULA, *The Theory of the Suspension Bridge*. Publications of International Association of Bridge and Structural Engineering (1936).

[4] J. B. JOHNSON, C. E. BRYAN and C. E. TURNEAURE, *The Theory and Practice of Modern Framed Structures*, Part 2. John Wiley (1911).

[5] S. P. TIMOSHENKO, Theory of suspension bridges, *J. Franklin Inst.* **235** (1943).

[6] S. O. ASPLUND, Column-beams and suspension bridges Analyzed by Green's Matrix. *Chalmers Tekniska Hogskolas Handlinger*. Number 204 (1958).

[7] T. J. POSKITT, Structural analysis of suspension bridges. *J. Struct. Div., Proc. Am. Soc. Civil Eng.* **92** (1966).

[8] S. A. SAAFIN, Theoretical analysis of suspension bridges, *J. Struct. Div., Proc. Am. Soc. Civil Eng.* **92** (1966).

[9] H. H. WEST and A. R. ROBINSON, A re-examination of the theory of suspension bridges. *Civil Engineering Series, Structural Research Series No. 322.* University of Illinois, Urbana, Illinois (1967).

[10] H. H. WEST and A. R. ROBINSON, Continuous method of suspension bridge analysis. *J. Struct. Div., Proc. Am. Soc. Civil Eng.* **94** (1968).

[11] N. M. NEWMARK, Numerical procedure for computing deflections, moments and buckling loads. *Trans. Am. Soc. Civil Eng.* **108** (1943).

[12] R. K. LIVESLEY, *Matrix Methods of Structural Analysis*. Pergamon Press (1964).

[13] J. MICHALOS and C. BIRNSTIEL, Movement of a cable due to changes in loading. *J. Struct. Div., Proc. Am. Soc. Civil Eng.* **86** (1960).

[14] C. H. THORNTON and C. BIRNSTIEL, Three-dimensional suspension structures. *J. Struct. Div., Proc. Am. Soc. Civil Eng.* **93** (1967).


## APPENDIX—EQUATIONS OF EQUILIBRIUM

In this Appendix, the basic equations of equilibrium for the cable-hanger system are derived by applying the principle of minimum potential energy. Definitions of terms already introduced in the text are not repeated here; however, all new terms are defined.

Taking $V_T$ as the total potential energy of the system and $\phi_i$ as one of the $m$ admissible displacements, we have the following $m$ equations of equilibrium:

$$\frac{\partial V_T}{\partial \phi_i} = 0 \qquad (i = 1, 2, \ldots, m). \tag{17}$$

The total potential energy is composed of two separate parts

$$V_T = U_T + \Omega_T \tag{18}$$

where $U_T$ is the total strain energy stored and $\Omega_T$ is the potential energy of the external loads.

Referring to Figs. 1 and 2, we have

$$U_T = \sum_{i=1}^{n} U_{if} + \sum_{i=2}^{n} U_{lif} + \tfrac{1}{2}(K_{H1}u_1^2 + K_{V1}v_1^2 + K_{H,n+1}u_{n+1}^2 + K_{V,n+1}v_{n+1}^2) \tag{19}$$

where $U_{if}$ and $U_{lif}$ refer to the strain energy in the final deformed configuration for the main cable and the hanger elements, respectively. The strain energy of the $i$th bar, $U_{if}$, in its deformed configuration is given by

$$U_{if} = \frac{E_i A_i (e_{id} + e_{il} - e_{it})^2}{2L_{i0}} \tag{20}$$

where $E_i$ is the modulus of elasticity, $A_i$ is the cross-sectional area, $e_{id}$ is the initial (generally dead load) elongation, $e_{il}$ is the additional elongation of the bar caused by the displacements associated with live load and temperature change, $e_{it}$ is the direct change in length caused by temperature change and $L_{i0}$ is the original bar length. All these quantities relate to the $i$th bar. The elongation $e_{il} = L_{if} - L_{id}$, where $L_{if}$ is the bar length in its deformed position and $L_{id}$ is the dead load length. Expressing $L_{if}$ in terms of the displacements shown in Fig. 2, we obtain

$$\begin{aligned} U_{if} = \frac{E_i A_i}{2L_{i0}} \Bigg[ & \frac{h_{id}^2(u_{i+1}-u_i)^2}{L_{id}^2} + \frac{2h_{id}r_{id}(u_{i+1}-u_i)(v_{i+1}-v_i)}{L_{id}^2} \\ & + \frac{r_{id}^2(v_{i+1}-v_i)^2}{L_{id}^2} + \frac{(e_{id}-e_{it})(u_{i+1}-u_i)^2}{L_{id}} + \frac{(e_{id}-e_{it})(v_{i+1}-v_i)^2}{L_{id}} \\ & + \frac{2(e_{id}-e_{it})h_{id}(u_{i+1}-u_i)}{L_{id}} + \frac{2(e_{id}-e_{it})r_{id}(v_{i+1}-v_i)}{L_{id}} \\ & - \frac{h_{id}^2(e_{id}-e_{it})(u_{i+1}-u_i)^2}{L_{id}^3} - \frac{2(e_{id}-e_{it})h_{id}r_{id}(u_{i+1}-u_i)(v_{i+1}-v_i)}{L_{id}^3} \\ & - \frac{(e_{id}-e_{it})r_{id}^2(v_{i+1}-v_i)^2}{L_{id}^3} - 2L_{id}\{L_{id}-(e_{id}-e_{it})\}R_i + (e_{id}-e_{it})^2 \Bigg] \end{aligned} \tag{21}$$

where $h_{id}$ and $r_{id}$ are the horizontal and vertical projections, respectively, of the $i$th bar in the dead load position, and

$$\begin{aligned} R_i = \sqrt{(1+X_i)} - \Bigg\{ 1 & + \frac{(u_{i+1}-u_i)^2}{2L_{id}^2} + \frac{(v_{i+1}-v_i)^2}{2L_{id}^2} + \frac{h_{id}(u_{i+1}-u_i)}{L_{id}^2} + \frac{r_{id}(v_{i+1}-v_i)}{L_{id}^2} \\ & - \frac{h_{id}^2(u_{i+1}-u_i)^2}{2L_{id}^4} - \frac{h_{id}r_{id}(u_{i+1}-u_i)(v_{i+1}-v_i)}{L_{id}^4} - \frac{r_{id}^2(v_{i+1}-v_i)^2}{2L_{id}^4} \Bigg\} \end{aligned}$$

and

$$X_i = \frac{(u_{i+1}-u_i)^2}{L_{id}^2} + \frac{(v_{i+1}-v_i)^2}{L_{id}^2} + \frac{2h_{id}(u_{i+1}-u_i)}{L_{id}^2} + \frac{2r_{id}(v_{i+1}-v_i)}{L_{id}^2}.$$

An expression for $U_{lif}$ can be similarly derived. Note that in equation (21) the strain energy has the linear and quadratic displacement terms explicitly separated. All higher order displacement terms are contained in $R_i$. This form is convenient because the differentiation indicated in equation (17) will yield equations with a linear part separated from a nonlinear part.

Again, with the aid of Figs. 1 and 2, we have as the potential energy of external loads

$$\Omega_T = \Omega_d - \sum_{i=1}^{n+1} (W_{Vi}+Q_{Vi})v_i + (W_{Hi}+Q_{Hi})u_i - \sum_{n=2}^{n} (W_{Vbi}+Q_{Vbi})v_{bi} \tag{22}$$

where $\Omega_d$ is the potential energy at the initial configuration.

At a typical station $i$ along the cable, the differentiation indicated in equation (17) is performed with respect to $u_i$, $v_i$ and $v_{bi}$ to yield, respectively, the equations for horizontal equilibrium at point $i$, vertical equilibrium at point $i$ and vertical equilibrium at point $bi$.

For example, $\partial V_T/\partial u_i = 0$ yields, after some manipulation

$$-\alpha_h u_h + (\alpha_h + \alpha_i + \alpha_{li} + K_{Hi})u_i - \alpha_i u_j - \beta_h v_h + (\beta_h + \beta_i + \beta_{li})v_i - \beta_i v_j - \beta_{li} v_{bi} + N_{Hi}$$

$$= \left(\frac{K_i e_{id} h_{id}}{L_{id}} - \frac{K_h e_{hd} h_{hd}}{L_{hd}} + \frac{K_{li} e_{lid} h_{lid}}{L_{lid}}\right) + W_{Hi} + Q_{Hi} + Q^t_{Hi}. \tag{23}$$

Similarly, $\partial V_T/\partial v_i = 0$ and $\partial V_T/\partial v_{bi} = 0$ produce, respectively,

$$-\beta_h u_h + (\beta_h + \beta_i + \beta_{li})u_i - \beta_i u_j - \gamma_h v_h + (\gamma_h + \gamma_i + \gamma_{li} + K_{Vi})v_i - \gamma_i v_j - \gamma_{li} v_{bi} + N_{Vi}$$

$$= \left(\frac{K_i e_{id} r_{id}}{L_{id}} - \frac{K_h e_{hd} r_{hd}}{L_{hd}} + \frac{K_{li} e_{lid} r_{lid}}{L_{lid}}\right) + W_{Vi} + Q_{Vi} + Q^t_{Vi} \tag{24}$$

and

$$-\beta_{li} u_i - \gamma_{li} v_i + \gamma_{li} v_{bi} + N_{Vbi} = \left(-\frac{K_{li} e_{lid} r_{lid}}{L_{lid}}\right) + W_{Vbi} + Q_{Vbi} + Q^t_{Vbi} \tag{25}$$

where the subscripts $h = (i-1)$ and $j = (i+1)$ and

$$\alpha_k = K_k \left\{\frac{h_{kd}^2}{L_{kd}^2} + \frac{(e_{kd} - e_{kt})}{L_{kd}} - \frac{h_{kd}^2 (e_{kd} - e_{kt})}{L_{kd}^3}\right\} \qquad (k = h, i, li)$$

$$\beta_k = K_k \left\{\frac{h_{kd} r_{kd}}{L_{kd}} - \frac{h_{kd} r_{kd} (e_{kd} - e_{kt})}{L_{kd}^3}\right\} \qquad (k = h, i, li)$$

$$\gamma_k = K_k \left\{\frac{r_{kd}^2}{L_{kd}^2} + \frac{(e_{kd} - e_{kt})}{L_{kd}} - \frac{r_{kd}^2 (e_{kd} - e_{kt})}{L_{kd}^3}\right\} \qquad (k = h, i, li)$$

$$K_k = A_k E_k / L_{k0} \qquad (k = h, i, li)$$

$$N_{Hi} = \sum_k \left[-K_k L_{kd} \{L_{kd} - (e_{kd} - e_{kt})\} \frac{\partial R_k}{\partial u_i}\right] \qquad (k = h, i, li)$$

$$N_{Vi} = \sum_k \left[-K_k L_{kd} \{L_{kd} - (e_{kd} - e_{kt})\} \frac{\partial R_k}{\partial v_i}\right] \qquad (k = h, i, li)$$

$$N_{Vbi} = \sum_k \left[-K_k L_{kd} \{L_{kd} - (e_{kd} - e_{kt})\} \frac{\partial R_k}{\partial v_{bi}}\right] \qquad (k = h, i, li)$$

$$\left.\begin{aligned} Q^t_{Hi} &= -\frac{K_i e_{it} h_{id}}{L_{id}} + \frac{K_h e_{ht} h_{hd}}{L_{hd}} - \frac{K_{li} e_{lit} h_{lid}}{L_{lid}} \\ Q^t_{Vi} &= -\frac{K_i e_{it} r_{id}}{L_{id}} + \frac{K_h e_{ht} r_{hd}}{L_{hd}} - \frac{K_{li} e_{lit} r_{lid}}{L_{lid}} \\ Q^t_{Vbi} &= \frac{K_{li} e_{lit} r_{lit}}{L_{lid}} \end{aligned}\right\} \quad \text{Equivalent temperature loads.}$$

The bracketed term on the right-hand side of equation (23) represents the summation of the horizontal components of forces in all elements framing into point $i$. If the structure is in equilibrium in its initial configuration, then this will cancel $W_{Hi}$ exactly. Similarly, the bracketed terms in equations (24) and (25) cancel $W_{Vi}$ and $W_{Vbi}$, respectively. Thus, for a structure originally in equilibrium, the right-hand sides of equations (23–25) contain only live load and temperature loads.

(*Received* 3 *August* 1972; *revised* 26 *February* 1973)

**Абстракт**—Дается формулировка задачи в дискретной форме для расчета подвешенных мостов. Уравнения равновесия, которые вообще нелинейны, выряжены в перемещениях, решаются методом Ньютона—Рафсона. Учитывается линейное решение начальных задач. Численные трудности требуют применения схемы пропуска для каждой линеаризации. Даются численные задачи как для усиленных так и неусиленных конструкций. Сравниваются результаты с поисками других исследователей. Исследуются эффекты пространственной подвески на результаты, специально, в концевых районах жестких связей.